COMPUTATIONAL ANALYSIS OF TURBULENT FORCED CONVECTION IN A CHANNEL WITH STAGGERED CORRUGATED BAFFLES

Younes Menni*, Ahmed Azzi, Chafika Zidani
Research Unit of Materials and Renewable Energies (URMER),
Department of Physics, Faculty of Sciences, Abou Bekr Belkaid University,
BP 119-13000-Tlemcen
**Corresponding author. E-mail: Youtifa_URMER.Physic@hotmail.fr*
Reçu le:25/02/2015 Accepté le: 27/06/2015

Abstract
A computational analysis of steady turbulent forced convection flow in a two- dimensional isothermal-wall rectangular channel fitted with lower and upper wall-mounted corrugated baffles is carried out in the present work. The governing equations based on the SST k-ω model used to describe the turbulence, are solved by the finite volume approach using the SIMPLE algorithm. The velocity and temperature fields, the temperature profiles, as well as the Nusselt number distribution were presented for a typical case.
Keywords: *Turbulent forced convection - Corrugated baffles - Finite volume method.*

Résumé
Cette étude porte sur l'analyse computationnelle de l'écoulement turbulent et du transfert de chaleur par convection forcée stationnaire à l'intérieur d'un canal bidimensionnel de section rectangulaire, muni des chicanes ondulées attachées en chevauchement dans les parois isothermes mères de la conduite. Les équations gouvernantes, basées sur le modèle k-ω SST, sont résolues par la méthode des volumes finis à l'aide de l'algorithme SIMPLE. Les champs de vitesse et de température, les profils de température ainsi que la distribution du nombre de Nusselt ont été présentés pour un cas d'exemple type.
Mots-clés: *Convection forcée turbulent - Chicanes ondulées - Méthode des volumes.*

1. INTRODUCTION

One of the essential problems concerning the use of solar energy is the small thermal exchange realized with the air in the dynamic vein of the solar collector. These exchanges do not allow the best performance or the best thermal efficiency of these systems. On the other hand, few studies have shown the heat transfer enhancement can be achieved by creating longitudinal vortices in the flow. These vortices are produced by introducing an obstacle in the flow,

known as a vortex generator. The pressure difference across the vortex generator causes flow separation and induces a vortex downstream. The vortex creates a rotating motion within the flow stream, which causes a rapid transfer of fluid parcels to and from the heat transfer surface. Baffles and fins submitted to laminar and turbulent flows have being analyzed in the recent years by several authors, using numerical (Nasiruddin and Kamran Siddiqui [1], Sripattanapipat and Promvonge [2], Benzenine et al. [3], and Dong et al. [4]) and/or experimental (Demartini et al. [5], Karwa and Maheshwari [6], Sriromreun et al. [7], and Wen et al. [8]) techniques. The results show that he flow is characterized by strong deformation and large recirculation regions. In general, convective Nusselt number and pressure loss increase with the Reynolds number.

Most of the investigations, cited above, have focused on fluid flow and heat transfer for baffle height and spacing ratios for vertical or inclined, solid or porous, flat or shaped baffles. In the present simulation, the numerical computations for two-dimensional convective turbulent flow over the corrugated baffles mounted repeatedly on two opposite heated walls of a rectangular channel are conducted with the main aim being to examine the changes in the flow structure and heat transfer characteristics.

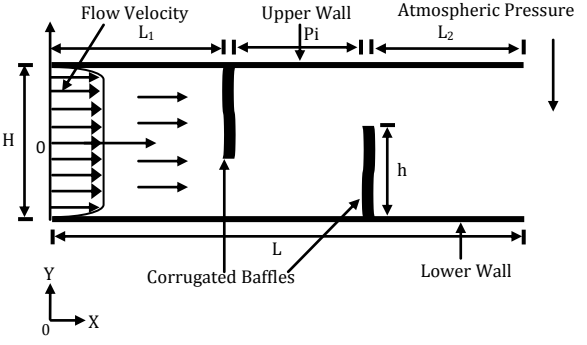

Fig. 1. Physical model with the corrugated baffles.

2. DESCRIPTION OF THE PROBLEM

Two-dimensional turbulent forced convection flow in a heated rectangular duct with a corrugated baffle pair is numerically simulated. The schematic configuration and computational domain are plotted in figure 1. The system consists of air flow moving through a rectangular channel provided with two corrugated baffles in turbulent conditions. Two different corrugated baffle configurations were considered in this investigation study, which are referred as cases A and B. In case A, a baffle corrugated towards the upstream end was considered (see Fig. 2a) and in case B, a baffle corrugated towards the downstream end was considered (see Fig. 2b).

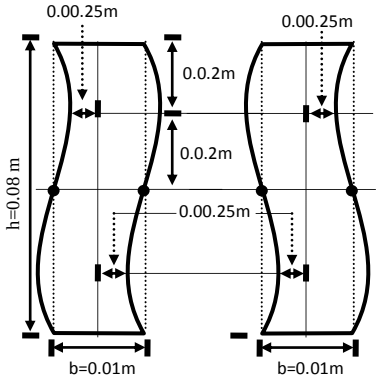

Fig. 2. (a) case A with a corrugated-upstream baffle, and (b) case B with a corrugated-downstream baffle.

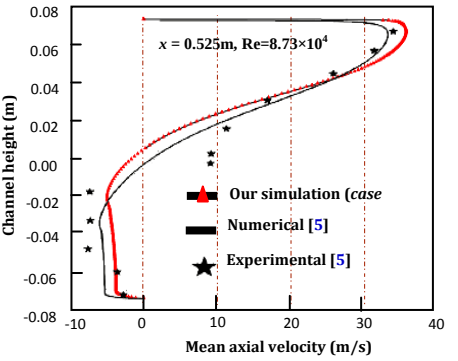

Fig. 3. Validation plot of the axial velocity distribution with reported data, near the channel outlet, Re=8.73×10^4.

3. MATHEMATICAL MODELING

The numerical fluid flow and heat transfer in the rectangular channel is developed under the following assumptions: (1) Steady two-dimensional flow and heat transfer, (2) The flow is turbulent and incompressible, (3) Constant fluid properties, (4) Body forces, viscous dissipation and radiation heat transfer are ignored.
Based on the above assumptions, the channel flow is governed by continuity, Navier–Stokes and energy equations, respectively

$$\nabla \vec{V} = 0 \quad (1)$$

$$\rho\left(\vec{V}.\nabla\vec{V}\right) = -\nabla P + \mu_f \nabla^2 \vec{V} \quad (2)$$

$$\rho C_p \left(\vec{V}.\nabla T\right) = K_f \nabla^2 T \quad (3)$$

The Shear Stress Transport k-ω model is selected to use in prediction of this complex flow. The SST k-ω model is defined by two transport equations, one for the turbulent kinetic energy, k and the other for the specific dissipation rate ω, as given below

$$\frac{\partial}{\partial x_i}(\rho k u_i) = \frac{\partial}{\partial x_j}\left(\Gamma_k \frac{\partial k}{\partial x_j}\right) + G_k - Y_k + S_k \quad (4)$$

$$\frac{\partial}{\partial x_i}(\rho \omega u_i) = \frac{\partial}{\partial x_j}\left(\Gamma_\omega \frac{\partial \omega}{\partial x_j}\right) + G_\omega - Y_\omega + D_\omega + S_\omega \quad 5)$$

where

$$G_k = -\rho \overline{u_i' u_j'} \frac{\partial u_j}{\partial x_i} \quad \text{and} \quad G_\omega = \alpha \frac{\omega}{k} G_k \quad (6)$$

$$\Gamma_k = \mu + \frac{\mu_t}{\sigma_k} \quad \text{and} \quad \Gamma_\omega = \mu + \frac{\mu_t}{\sigma_\omega} \quad (7)$$

In these equations, $\vec{V}$ is the velocity vector, P represents the pressure, ρ, μ_f, K_f and C_p are respectively the density, the dynamics viscosity, the thermal conductivity and specific heat of fluid, x_i and x_j are the spatial coordinates, G_k represents the generation of turbulence kinetic energy due to mean velocity gradients, G_ω represents the generation of ω, Γ_k and Γ_ω represent the effective diffusivity of k and ω, respectively. Y_k and Y_ω represent the dissipation of k and ω due to turbulence, respectively. D_ω represents the cross-diffusion term, S_k and S_ω are user-defined source terms.

The governing equations were discretized by the QUICK scheme [9], decoupling with the SIMPLE-algorithm and solved using a finite volume approach [9]. The solutions were converged when the normalized residual values were less than 10^{-7} for all variables but less than 10^{-9} only for the energy equation. The hydrodynamic boundary conditions are chosen according to the experimental work of Demartini et al. [5]. The thermal boundary conditions are chosen according to the numerical work of Nasiruddin and Kamran Siddiqui [1]. In the entrance region, a uniform velocity distribution is applied. No-slip and impermeability boundary conditions are imposed at the walls. A constant temperature of 102°C was applied on the entire wall as the thermal boundary condition. The

temperature of air was set equal to 27°C at the channel inlet. The Reynolds number of the experiments [5] is Re=8.73×10⁴, defined as

$$\mathrm{Re} = \frac{\rho \overline{U} D_h}{\mu} \tag{8}$$

The local Nusselt number, Nu_x is evaluated as follows

$$Nu_x = \frac{h_x D_h}{\lambda_f} \tag{9}$$

The average Nusselt number, Nu_{av} can be obtained by

$$Nu_{av} = \frac{1}{L}\int Nu_x \partial x \tag{10}$$

where $\overline{U}$ is the entrance velocity, 7.8 m/s, and D_h is the hydraulic diameter of the channel, equal to 0.167 m, h_x represents the local convective heat transfer coefficient.

3.1. Grid sensitivity

To obtain grid independence solution, the number of cells ($N_x \times N_y$) is varied between 270×145 and 420×220 meshes. It is found that the percentage difference in heat transfer coefficient between the results of grid system of about 270×145 and 420×220 is on average 0.75% at the Reynolds number Re=8.73×10⁴. Considering both convergent time and solution precision, the grid system of 270×145 cells with finer resolution near the walls was adopted for the computational model.

3.2. Numerical validation

For the numerical simulations presented in this work, we refer to the experimental work done by Demartini et al. [5], who studied the baffles with a flat rectangular shape. The geometric dimensions of the system are: length of the channel L=0.554m, height H=0.146m, thickness of the two baffles b=0.01m, distance between baffles Pi=0.142m, the first is attached to the upper wall of the channel at distance of L_1=0.218m and the second inserted to the lower wall at L_2=0.37m from the entrance.

A comparison of numerical and experimental results of axial velocity profiles after the second baffle, near the channel outlet is given in figure 3. The Figure shows the comparison between our results and those obtained by Demartini et al. [5]. At a position

x=0.525m, it is clear from the figure that the modeling results are in good agreement with the Demartini's experimental results [5].

4. RESULTS AND DISCUSSION

The flow structure in the corrugated baffle presence could be easily discerned by considering the axial velocity field plots as depicted in figure 4 a and b for the cases A (corrugated-upstream baffles) and B (corrugated-downstream baffles), respectively. Here the flow around the baffle module is presented at different Re. In all cases, the results show very low velocities adjacent to the corrugated baffles. In the regions downstream of both baffles, recirculation cells with very low velocity values are observed. In the regions between the tip of the corrugated baffles and the channel walls, the velocity is increased. Due to the changes in the flow direction produced by the considered baffles, the highest velocity values appear near the upper channel wall with an acceleration process that starts just after the second corrugated baffle.

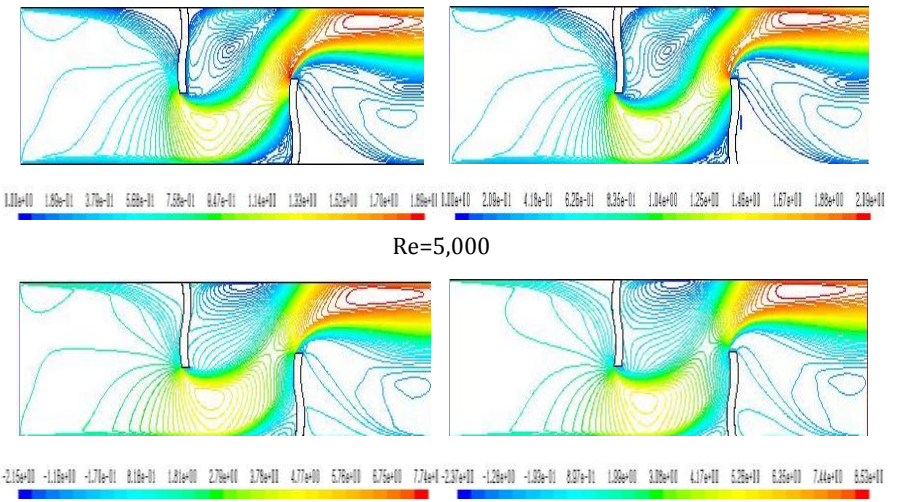

Fig. 4. Axial velocity contours at different Re values for cases: (a) corrugated-upstream, and (b) corrugated-downstream baffles.

The comparison of velocity distribution for the two treated cases at various Reynolds number values shows that the flow is

characterized by strong deformations and large recirculation regions. The results also show that the air flow is accelerating in its main direction from left towards right-hand side by increasing the recirculation zones size hence the length of these regions of recycling is proportional to the increase in the Reynolds number. It is also noticed that the hydrodynamic performance of the corrugated-downstream baffle (case B) is found to be higher than that of corrugated-upstream baffle (case A) for all Re used.

The temperature distribution along the channel at different Re values for cases A and B is plotted in figure 5 a and b, respectively.

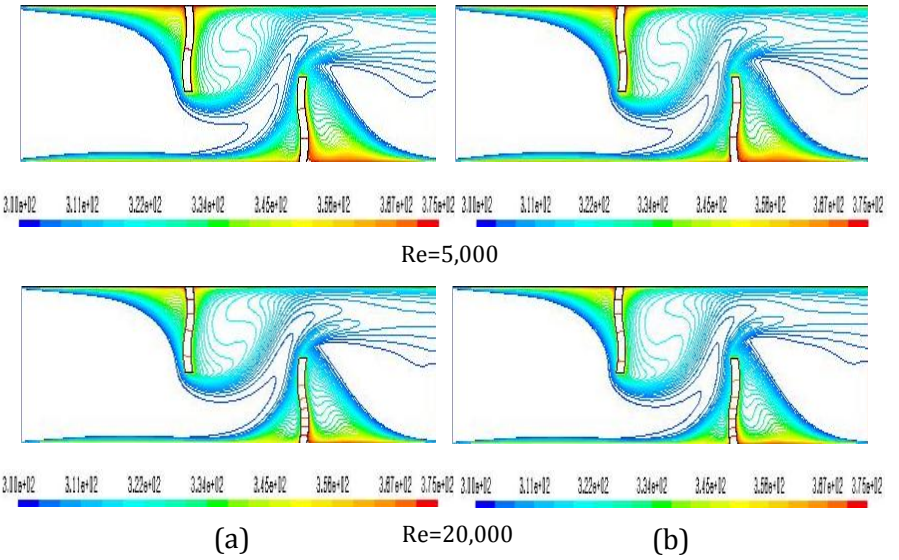

Fig. 5. Temperature contours at different Re values for cases: (a) corrugated-upstream and (b) corrugated-downstream baffles.

For all cases, the plot shows that the fluid temperature in the recirculation region is significantly high as compared to that in the same region of no baffle case. This means that the recirculation zone provide a significant influence on the temperature field, because they can induce better fluid mixing between the wall and the core regions, leading to a high temperature gradient along the heating channel wall. The isotherm contours obtained for different Re values presented in figure 5 also show that that when the Re increases, the isotherm contours become thoroughly denser, which

yields to the removal of higher quantities of energy from corrugated baffle faces. The graphical representations of the temperature variation as a function of Re for various baffles in different channel sections, at x=0.255m and x=0.285m from entrance, are shown in figure 6 a and b, respectively. These results certify that the heat exchange between the working fluid and the heated walls in the channel with two different corrugated baffle configurations is more important with low flow Reynolds numbers.

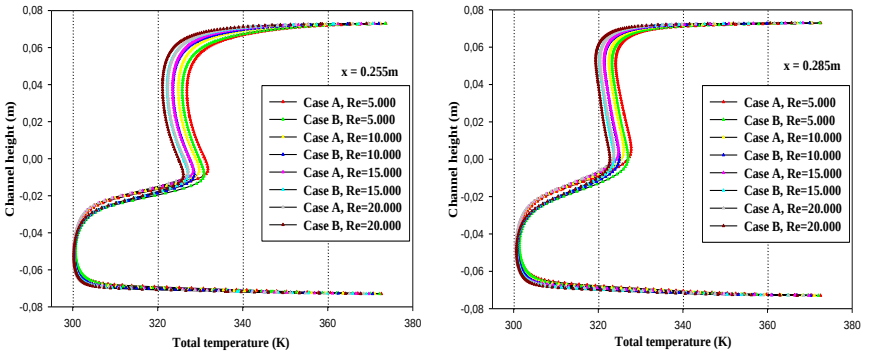

(a) (b)

Fig. 6: Variation of temperature profiles with Re for configurations A and B at positions: (a) x=0.255m, and (b) x=0.285m.

It is clear that for high Re values, the fluid temperature significantly decreases i.e., there exists an inverse proportionality between increasing flow Re number and the temperature in each channel cross section. Additionally, according to analysis of our results on the axial velocity profiles (see Fig. 4) and the temperature profiles for different sections (see Fig. 6), it is found that the fluid temperature is related to the flow velocity. When the incoming flow velocity is high, the heat exchange time is less, and hence decreasing of the bulk temperature. The heat transfer coefficient is presented in this study in terms of local and average Nusselt numbers for the corrugated baffles duct in figure 7 a and b, respectively. Figure 7a presents the local heat transfer results for airflow in the channel for two different baffle cases (A and B). In the figure, the Nu_x values are related as a function of Re along the heated top wall. In both cases, the first corrugated baffle is attached to the heated top surface, located at x=0.218m. In the figure, it is

worth noting that the largest variations are found near the tip of the corrugated baffle, due to the strong velocity gradients in that region, and the smallest value in the region around the upper wall baffle for all cases. It is visible that the Nu_x distribution trends are nearly similar for all corrugated baffle configurations. The use of corrugated-downstream baffle shows better Nu_x distribution values over the corrugated-upstream baffle at all locations. In addition, in the figure, it is interesting to note that the Nu_x value tends to increase with the rise of flow Re values for all baffles used.

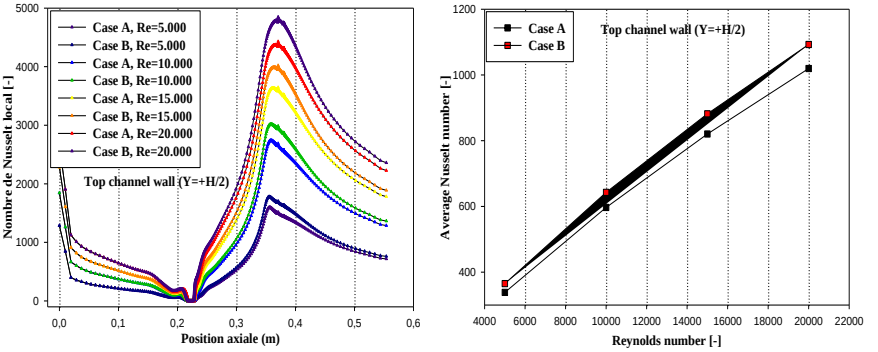

(a) (b)

Fig. 7. Variation of (a) Nu_x and (b) Nu_{av} with Re along the upper channel wall for various baffles (Cases A and B).

The variation of average Nusselt number, Nu_{av} is also presented in the figure (see Fig. 7b) which shows that the Nu_{av} increases with the increase of Re. In all cases, the channel with baffles corrugated towards the downstream end (case B) give higher values of Nu_{av} than that for the channel with baffles corrugated towards the upstream end (case A) due to the induction of high reverse flow and thin boundary layer, leading to higher temperature gradients.

5. CONCLUSION

A numerical study of the turbulent forced convection in a rectangular channel with two corrugated baffles has been conducted. The computational results reveal that the thermal performance of the baffle corrugated towards the downstream side

is found to be higher than that of the baffle corrugated towards the upstream side for all Re values used. For two treated baffle cases, the convective Nusselt enhancement increases with increasing the flow Re number. The above results suggest that a significant heat transfer enhancement in a heat exchanger duct can be achieved by introducing corrugated-downstream baffles into the flow.

References

[1] Nasiruddin, M.H. Kamran Siddiqui, Heat transfer augmentation in a heat exchanger tube using a baffle, Int. J. Heat and Fluid Flow 28 (2006) 318-328.
[2] S. Sripattanapipat, P. Promvonge, Numerical analysis of laminar heat transfer in a channel with diamond-shaped baffles, Int. Comm. Heat & Mass Transf. 36 (2009) 32-38.
[3] H. Benzenine, R. Saim, S. Abboudi, O. Imine, Numerical study on turbulent flow forced-convection heat transfer for air in a channel with waved fins, Mechanika 19(2) (2013) 150-158.
[4] C. Dong, Y.-P. Chen, J.-F. Wu, Flow and heat transfer performances of helical baffle heat exchangers with different baffle configurations, Applied Thermal Engineering 80 (2015) 328-338.
[5] L.C. Demartini, H.A. Vielmo, S.V. Möller, Numeric and experimental analysis of the turbulent flow through a channel with baffle plates J. the Braz. Soc. of Mech. Sci. & Eng. 26(2) (2004) 153-159.
[6] R. Karwa, B.K. Maheshwari, Heat transfer and friction in an asymmetrically heated rectangular duct with half and fully perforated baffles at different pitches, Int. Comm. in Heat and Mass Transfer 36 (2009) 264-268.
[7] P. Sriromreun, C. Thianpong, P. Promvonge, Experimental and numerical study on heat transfer enhancement in a channel with z-shaped baffles, Int. Comm. Heat & Mass Transfer 39 (2012) 945-952.
[8] J. Wen, H. Yang, S. Wang, Y. Xue, X. Tong, Experimental investigation on performance comparison for shell-and-tube heat exchangers with different baffles, Int. J. Heat and Mass Transfer 84 (2015) 990-997.
[9] S.V. Patankar, Numerical heat transfer and fluid flow, Hemisphere Publishing Corporation, New York, 1980.